400G MIMO-FSO Transmission with Enhanced Reliability Enabled by Joint LDPC Coding

Marco A. Fernandes, Paulo P. Monteiro and Fernando P. Guiomar

Instituto de Telecomunicações and University of Aveiro, Campus Universitário de Santiago, 3810-193, Portugal.
marcofernandes@av.it.pt

Abstract *We experimentally demonstrate error-free MIMO-FSO transmission of 2×200 Gbps, with joint LDPC coding between the signals, leading to an increase in tolerated channel power loss of 2 dB. Moreover, we show enhanced communication reliability in Gamma-Gamma MIMO-FSO systems.*

Introduction

Owing to their high bandwidth, low-complexity, license-free spectrum and ease-of-deployment, FSO systems have been recently proposed for a variety of scenarios, from 5G and beyond-5G architectures [1], to inter- and intra-datacenter communications [2]. However, atmospheric turbulence remains as the main bottleneck for FSO communications [3], hindering its widespread commercial deployment. The performance volatility of FSO demands the use of forward error correction (FEC) to enable error-free transmission, while accounting for fluctuations on link condition [4]. Moreover, in multiple-input multiple-output (MIMO)-FSO systems, the overall performance and reliability of the FSO link can be improved if proper joint-coding is performed [5].

The popularity of soft-decision FEC continues to increase in coherent optical systems, where low-density parity check (LDPC) codes stand out [6]. These codes are not only being used in all-fiber systems, but also being proposed for optical wireless systems [7] and for joint coding/decoding in massive MIMO scenarios [8]. Despite the plethora of coding schemes that have already been proposed for MIMO-FSO systems [5], there is still a lack of experimental demonstration of actual post-FEC BER measurements exposing the diversity gain, enhanced reliability and practical feasibility of the MIMO-FSO concept.

In this work, we experimentally demonstrate the transmission of 2×200 Gbps over a jointly LDPC-coded FSO link, and we report an increase of approximately 2 dB in terms of overall resilience to power losses/fluctuations emulated according to well-known atmospheric channel models. Stemming from this MIMO diversity gain, we demonstrate a significant enhancement of communication reliability, boosting the practical feasibility of high-capacity FSO systems.

2× 2 Jointly-Coded LDPC Scheme

The proposed 2×2 joint LDPC-coding concept is presented in Fig. 1. The transmitted bits originating from two different logic channels are firstly combined in a parallel-to-serial (P/S) block. Then, these interleaved bits are encoded by an LDPC coder with a given FEC rate. To benefit from the FSO spatial diversity, the coded bits are again de-interleaved by a serial-to-parallel (S/P) block, and independently modulated by quadrature amplitude modulation (QAM) mappers. After transmission over disjoint FSO links, the two received signals are processed and demodulated in the respective QAM demappers. At that point, pre-FEC bit-error rate (BER) can be calculated for each link. The demapped bits are combined again in the P/S block, where an average pre-FEC BER of the joint channel can be measured, and then sent to the LDPC decoder, which attempts at performing error correction. From the decoded bits, a post-FEC BER can be evaluated, by comparing the serialized transmitted bits with the corresponding decoded received bits. The main aim of the proposed joint coding scheme is to make the post-FEC BER sensible to the average pre-FEC BER of the disjoint links, thereby enabling to average out the atmospheric turbulence distortion across the two FSO links. If an overall error-free post-FEC BER is guaranteed, then also the individual bit tributaries of channels 1 and 2 can be retrieved with no errors, by simply de-interleaving the serialized decoded bits.

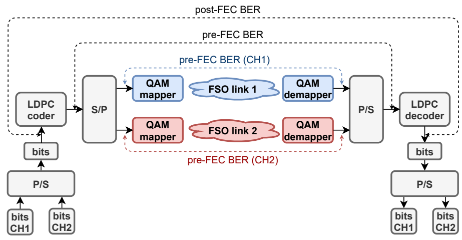

Fig. 1: 2×2 joint LDPC coding and decoding scheme.

Experimental Setup

The experimental setup is depicted in Figure 2. At the transmitter, we take the bitstreams of two 30 Gbaud independent signals and apply the joint LDPC coding in accordance with Fig. 1, with an FEC rate of 5/6. The de-interleaved encoded

978-1-6654-3868-1/21/$31.00 ©2021 IEEE

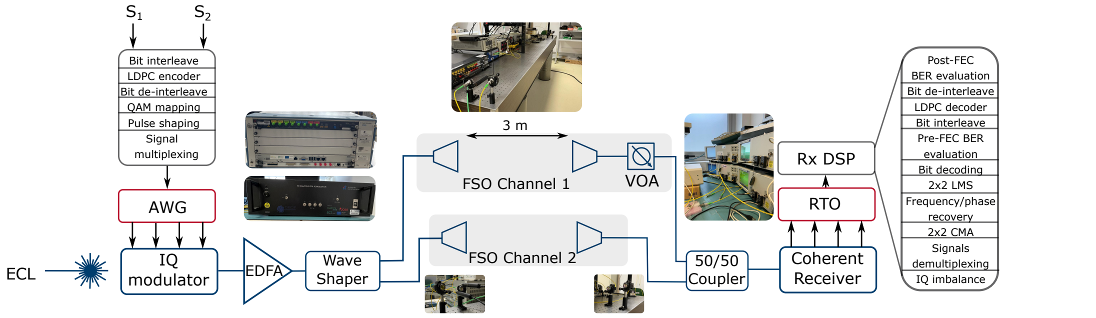

ECL: External Cavity Laser; **S_1**: Signal 1; **S_2**: Signal 2; **LDPC**: Low-Density Parity-Check; **QAM**: Quadrature Amplitude Modulation; **AWG**: Arbitrary Waveform Generator; **EDFA**: Erbium-Doped Fiber Amplifier; **FSO**: Free-Space Optics; **VOA**: Variable Optical Attenuator; **RTO**: Real-Time Oscilloscope; **CMA**: Constant Modulus Algorithm; **LMS**: Least-Mean Squares; **FEC**: Forward Error Correction; **BER**: Bit-Error Rate.

Fig. 2: Experimental setup used to demonstrate the 2×2 FSO-link reliability gains when using joint LDPC encoding between two independent signals.

bitstreams are then mapped into 16QAM constellations. The two signals are root-raised cosine shaped, with a 0.05 roll off. The two signals are generated by frequency multiplexing in a single arbitrary waveform generator (AWG) with 120GSa/s and an analog bandwidth of ∼45 GHz (Keysight M8194A). A dual-polarization IQ modulator (35 GHz bandwidth) modulates the electrical signal onto the optical carrier provided by an external cavity-laser (ECL) with 13 dBm output power. The optical signal is then amplified by an erbium-doped fiber amplifier (EDFA). Next, a waveshaper (Finisar WS4000S) has the function of separating the frequency multiplexed signals. Each one of these signals is sent to a different FSO channel (both FSO-links have a length of 3 m). In one of the channels (CH1), we add a variable optical attenuator (VOA) that is used to emulate the FSO power-losses induced by atmospheric turbulence. Each free-space link consists of a seamless fiber-FSO link, where the interface between fiber core and free-space is performed by a fiber collimator (Thorlabs F810APC-1550) with 24 mm lens diameter, 0.24 numerical aperture and 0.0017° divergence angle. This architecture enables the existence of a FSO-link that does not introduce bandwidth limitations in the system. The received signals are then collected using a 50/50 optical coupler, and the resulting signal is sent to an optical coherent receiver with 40 GHz bandwidth. The electrical I and Q components are sampled and digitized by 4 real-time oscilloscopes, each one with 200 GSa/s sample rate and 70 GHz bandwidth (Tektronix DPO77002SX-R3). In the digital domain, typical digital signal processing (DSP) techniques are performed, starting by compensating for any IQ imbalance and frequency demultiplexing of each single-carrier signal. Each signal is then individually processed by the following DSP systems: 2×2 CMA-based adaptive equalization (15 taps), frequency and phase recovery, 2×2 LMS equalization (51 taps), bit decoding and pre-FEC bit-error-rate (BER) assessment. After merging the two estimated receiver-side bitstreams (as in Fig. 1), an LDPC decoder (5 iterations) is applied and the bits are finally de-interleaved, enabling to evaluate the post-FEC BER of each channel.

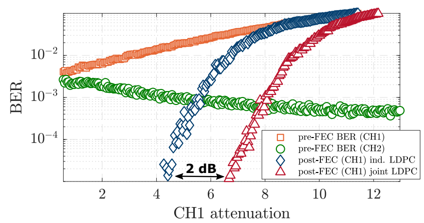

Fig. 3: Comparison of system performance with normal LDPC-encoding and with the proposed joint encoding.

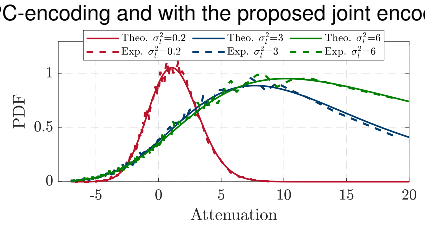

Fig. 4: Theoretical and practical probability density functions of the random attenuation applied to CH1.

Experimental validation with a 2x2 FSO link

To perform the proposed LDPC joint coding validation, we tested the transmission of 2×30 Gbaud 16QAM signals through the MIMO-FSO testbed exposed in Fig. 2. To compare the robustness of each method, we used the VOA to sweep the attenuation introduced in CH1 and measured the pre-FEC and post-FEC BER of each channel, with independent and joint LDPC coding. The obtained results are depicted in Fig. 3. As one should expect, increasing the attenuation in CH1, will impose a performance degradation in this same channel. From this reason we see that the channel only supports a power-loss of ∼4 dB with normal independent LDPC encoding. For higher attenuations, the FEC coding is not enough to present an error-free transmission. We can also observe that the pre-FEC BER of the Channel 2 (CH2) improves as the CH1 has less power. This is due to having only one receiver for both signals, and so, the performance of the receiver will be improved for

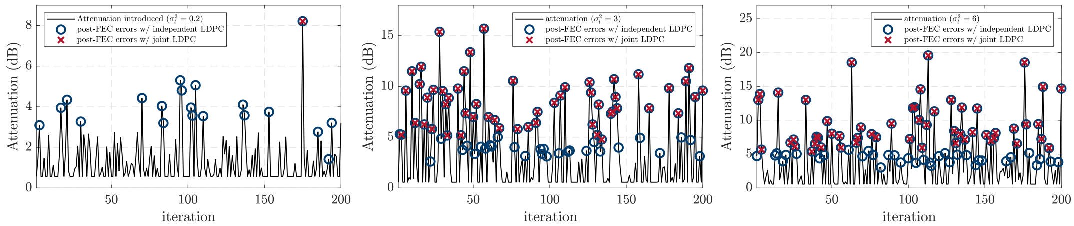

Fig. 5: Attenuation introduced to emulate the three different scenarios of atmospheric turbulence. It is also exposed the iterations where the a post-FEC BER with errors was present with independent coding (○), and joint coding (×)

the better channel, as the other becomes more irrelevant. Finally, the curve of post-FEC BER obtained with joint coding shows a 2 dB gain over typical encoding, which can be crucial in typical outdoor scenarios, where atmospheric turbulence can cause large power fluctuations.

Resilience to atmospheric turbulence

Several models have been proposed in the literature to model the effects of atmospheric turbulence in an FSO link. From those models, Gamma-Gamma (GG) has been widely used due to its capacity to model turbulence from the weak to the strong regime. This model was first proposed in [9] and considers that the probability density function (pdf) of the received irradiance (I_t) is:

$$p(I_t) = \frac{2(\alpha\beta)^{\frac{\alpha+\beta}{2}}}{\Gamma(\alpha)\Gamma(\beta)} I_t^{\frac{\alpha+\beta}{2}-1} K_{\alpha-\beta}(2\sqrt{\alpha\beta I_t}), I_t > 0, \tag{1}$$

where α is the effective number of large-scale eddies, β is the effective number of small-scale eddies, $K_{\alpha-\beta}(.)$ is the modified Bessel function of the second kind of order ($\alpha - \beta$) and lastly $\Gamma(.)$ is the Gamma function. Since α and β can be obtained from the Rytov variance (σ_l^2) we can extract the GG pdf directly from σ_l^2. The Rytov variance is widely used to classify the strength of the atmospheric turbulence, where weak turbulence is characterized by $\sigma_l^2 < 0.3$ and strong turbulence is characterized by $\sigma_l^2 \geq 5$.

In this sense, we decided to use the VOA of Fig. 2 to emulate a temporal power-fading following the GG model, to test the robustness towards atmospheric turbulence of the proposed joint LDPC scheme. Figure 4 shows the pdfs of the induced attenuation, as well as the corresponding theoretical GG function. Since statistically it is possible to induce some gain (attenuation below 0 dB), we decided to saturate the minimum attenuation to 0 dB. In these conditions, 3 scenarios were tested: i) weak-turbulence ($\sigma_l^2 = 0.2$), ii) moderate-turbulence ($\sigma_l^2 = 3$) and iii) strong-turbulence ($\sigma_l^2 = 6$).

We proceed by introducing the aforementioned attenuations in the system and measuring the gain of performing joint-LDPC coding between the channels. For each attenuation, the post-FEC BER was measured when applying independent LDPC coding and when using the proposed joint LDPC between channels. The results of the three turbulent scenarios are depicted in Fig. 5, which shows the attenuation introduced in each scenario (following the distributions of Fig. 4), and the realizations where a post-FEC BER with errors was measured. As expected, performing joint coding considerably increases the robustness of the FEC decoder, significantly reducing the number of occurrences with non-zero post-FEC BER.

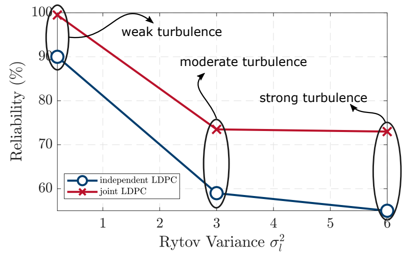

Fig. 6: Reliability of each encoding method as a function of the Rytov variance.

Finally, in Fig. 6 we show the overall reliability of the system as a function of the Rytov variance. For these results, we consider that the system is reliable only if the measured post-FEC BER is 0. When the system is under a weak-turbulence scenario, the system is quite reliable, presenting error-free transmission over 90% of the time. However, by introducing the joint coding scheme, the reliability increases considerably, exceeding 99%. As the Rytov variance increases, both reliabilities are reduced, however, the gain of introducing the joint coding increases.

Conclusion

In this work, we experimentally demonstrate the transmission of 2×200 Gbps through a MIMO-FSO link with reliability enhancement enabled by joint LDPC coding between the channels. The method is experimentally demonstrated in a Gamma-Gamma-like channel with considerable gains in communication reliability.

Acknowledgements

This work was partially supported by FEDER, through the CENTRO 2020 programme, project ORCIP (CENTRO-01-0145-FEDER-022141), and by FCT/MCTES through project FreeComm-B5G (UIDB/EEA/50008/2020). Fernando P. Guiomar acknowledges a fellowship from "la Caixa" Foundation (ID 100010434). The fellowship code is LCF/BQ/PR20/11770015. Marco Fernandes acknowledges a PhD fellowship from FCT. The fellowship code is 2020.07521.BD.

References

[1] A. O. Mufutau, F. P. Guiomar, M. A. Fernandes, A. Lorences-Riesgo, A. Oliveira, and P. P. Monteiro, "Demonstration of a hybrid optical fiber–wireless 5g fronthaul coexisting with end-to-end 4g networks", *Journal of Optical Communications and Networking*, vol. 12, no. 3, p. 72, Feb. 2020. DOI: 10.1364/jocn.382654.

[2] M. A. Fernandes, P. P. Monteiro, and F. P. Guiomar, "Single-wavelength terabit FSO channel for datacenter interconnects enabled by adaptive PCS", in *2021 Optical Fiber Communications Conference and Exhibition (OFC)*, 2021.

[3] H. Kaushal and G. Kaddoum, "Optical communication in space: Challenges and mitigation techniques", *IEEE Communications Surveys & Tutorials*, vol. 19, no. 1, pp. 57–96, 2017. DOI: 10.1109/comst.2016.2603518.

[4] H. G. Sandalidis, "Coded free-space optical links over strong turbulence and misalignment fading channels", *IEEE Transactions on Communications*, vol. 59, no. 3, pp. 669–674, 2011. DOI: 10.1109/TCOMM.2011.121410.090318.

[5] B. Mortada, H. S. Ghanem, R. S. Hammad, S. E.-D. N. Mohamed, A. Sedik, R. A. Eltaieb, W. El-Shafai, A. N. Z. Rashed, M. A. M. El-Bendary, M. S. F. Tabbour, G. M. E. Banby, A. A. Khalaf, A. E. A. Farghal, H.-d. H. Ahmed, G. A. Hussein, E.-S. M. El-Rabaie, I. M. Eldokany, M. I. Dessouky, A. A. Mohamad, O. Zahran, M. Elsabrouty, H. F. A. Hamed, G. M. Salama, S. E. El-Khamy, H. M. H. Shalaby, and F. E. A. El-Samie, "Optical wireless communication performance enhancement using hamming coding and an efficient adaptive equalizer with a deep-learning-based quality assessment", *Appl. Opt.*, vol. 60, no. 13, pp. 3677–3688, May 2021. DOI: 10.1364/AO.418438. [Online]. Available: http://ao.osa.org/abstract.cfm?URI=ao-60-13-3677.

[6] T. Gerard, H. Dzieciol, E. Sillekens, Y. Wakayama, A. Alvarado, R. I. Killey, P. Bayvel, and D. Lavery, "Coded modulation for 100g coherent epon", *Journal of Lightwave Technology*, vol. 38, no. 3, pp. 564–572, 2020. DOI: 10.1109/JLT.2019.2940889.

[7] B. Barua and S. P. Majumder, "Ldpc coded ofdm ow communication system with coherent optical receiver and rf synchronous demodulation under turbulent condition", in *2019 IEEE International Conference on Telecommunications and Photonics (ICTP)*, 2019, pp. 1–4. DOI: 10.1109/ICTP48844.2019.9041818.

[8] I. Hwang, H. J. Park, and J. W. Lee, "Ldpc coded massive mimo systems", *Entropy*, vol. 21, no. 3, 2019, ISSN: 1099-4300. DOI: 10.3390/e21030231. [Online]. Available: https://www.mdpi.com/1099-4300/21/3/231.

[9] M. A. Al-Habash, "Mathematical model for the irradiance probability density function of a laser beam propagating through turbulent media", *Optical Engineering*, vol. 40, no. 8, p. 1554, Aug. 2001. DOI: 10.1117/1.1386641.